

Orientation dependence and tension/compression asymmetry of shape memory effect and superelasticity in ferromagnetic $\text{Co}_{40}\text{Ni}_{33}\text{Al}_{27}$, $\text{Co}_{49}\text{Ni}_{21}\text{Ga}_{30}$ and $\text{Ni}_{54}\text{Fe}_{19}\text{Ga}_{27}$ single crystals

Y. Chumlyakov^{a,*}, E. Panchenko^a, I. Kireeva^a, I. Karaman^b, H. Sehitoglu^c,
H.J. Maier^d, A. Tverdokhlebova^a, A. Ovsvannikov^a

^a Siberian Physical Technical Institute, Novosobornaya sq. 1, Tomsk 634050, Russia

^b Department of Mechanical Engineering, Texas A&M University, College Station, TX 77843, USA

^c Department of Mechanical and Industrial Engineering, University of Illinois at Urbana-Champaign, Urbana, IL 61801, USA

^d University of Paderborn, Lehrstuhl für Wekstoffkunde, 33098 Paderborn, Germany

Received 26 May 2006; received in revised form 16 January 2007; accepted 9 February 2007

Abstract

In the present study the effects of crystal axis orientation, stress state (tension/compression) and test temperature on shape memory effect and superelasticity of $\text{Ni}_{54}\text{Fe}_{19}\text{Ga}_{27}$ (I), $\text{Co}_{40}\text{Ni}_{33}\text{Al}_{27}$ (II), $\text{Co}_{49}\text{Ni}_{21}\text{Ga}_{30}$ (III) (numbers indicate at.%) single crystals were investigated. The shape memory effect, the start temperature of superelasticity T_1 and the mechanical hysteresis $\Delta\sigma$ were found to be dependent on crystal axis orientation and stress state. Superelasticity was observed at $T_1 = A_f$ (A_f , reverse transformation-finish temperature) in tension/compression for [00 1]-oriented Ni–Fe–Ga crystals and in compression for [00 1]-oriented Co–Ni–Ga crystals, which all displayed a small mechanical hysteresis ($\Delta\sigma \leq 30$ MPa). An increase in $\Delta\sigma$ of up to 90 MPa in the Co–Ni–Al and the Co–Ni–Ga crystals lead to stabilization of the stress-induced martensite, and an increase in $T_1 = A_f + \Delta$. The maximal value of Δ (75 K) was found in [00 1]-oriented Co–Ni–Al crystals in tension. A thermodynamic criterion describing the dependencies of the start temperature of superelasticity T_1 on crystal axis orientation, stress state and the magnitude of mechanical hysteresis is discussed.

© 2007 Elsevier B.V. All rights reserved.

Keywords: Single crystals; Stress-induced martensite; Ferromagnetic shape memory alloys; Superelasticity

1. Introduction

In ferromagnetic alloys undergoing thermoelastic martensitic transformations (MT), large recoverable strains can be induced not only by mechanical stress and temperature, but also by a constant magnetic field. Ni_2MnGa alloys have been studied extensively as these exhibit the magnetic shape memory effect [1–4]. The phenomena of magnetoplasticity and magnetoelasticity was also experimentally established in [00 1]-oriented Ni_2MnGa single crystals under simultaneous action of external stress and magnetic field [1]. However, these alloys have low plasticity and are brittle under tension/compression when the high-temperature phase is present [1–3]. Recently developed ferromagnetic Co–Ni–Al, Co–Ni–Ga and Ni–Fe–Ga alloys provide

for good plasticity of the high-temperature phase as compared to Ni_2MnGa alloy and are considered as promising materials for various applications that make use of the magnetic shape memory effect, magnetoplasticity or magnetoelasticity [4–8]. For realization of large recoverable strain under the simultaneous action of external stress and magnetic field, the ferromagnetic crystals should combine low detwinning stresses in martensite, high magnetocrystalline anisotropy, small thermal and mechanical hysteresis and a high yield stress of the high-temperature phase [1]. However, a systematic study of the thermoelastic MT under cooling/heating and applied stress is still lacking for development of new ferromagnetic alloys of Co–Ni–Al, Co–Ni–Ga and Ni–Fe–Ga. Thus, the main purposes of this work was to investigate the effect of stress state (tension/compression) on the stress-induced MT, shape memory effect (SME) and superelasticity (SE) in new ferromagnetic $\text{Ni}_{54}\text{Fe}_{19}\text{Ga}_{27}$, $\text{Co}_{40}\text{Ni}_{33}\text{Al}_{27}$ (at.%) single crystals stressed along the [00 1] direction and to study the influence of crystal axis orientation on the

* Corresponding author. Tel.: +7 3822533209; fax: +7 3822533034.
E-mail address: chum@phys.tsu.ru (Y. Chumlyakov).

forementioned functional properties in $\text{Co}_{49}\text{Ni}_{21}\text{Ga}_{30}$ (at.%) single crystals under compression.

2. Experimental procedure

Single crystals of $\text{Ni}_{54}\text{Fe}_{19}\text{Ga}_{27}$, $\text{Co}_{40}\text{Ni}_{33}\text{Al}_{27}$, $\text{Co}_{49}\text{Ni}_{21}\text{Ga}_{30}$ (at.%) were grown by the Bridgman technique in an inert gas atmosphere. In the following these alloys will be referred to as type I (Ni–Fe–Ga), type II (Co–Ni–Al) and type III (Co–Ni–Ga) crystals. Electro-discharge machining was utilized to cut regular dog-bone shaped flat tensile specimens with nominal dimensions of $16\text{ mm} \times 2.5\text{ mm} \times 1.5\text{ mm}$ in the gauge section and rectangular compression specimens with nominal dimension of $3\text{ mm} \times 3\text{ mm} \times 6\text{ mm}$. Mechanical grinding followed by an electrochemical polish (210 ml H_3PO_4 + 25 ml Cr_2O_3 at $T=293\text{ K}$, $U=20\text{ V}$) were employed to remove any processing-affected surface layer. The orientation of the crystal axis was determined in the austenitic state with a DRON-3 X-ray diffractometer an Fe $\text{K}\alpha$ radiation. The type I and type III single crystals were investigated in the as-grown state. The high-temperature phase of these crystals (without heat treatment) was found to have a L_{21} structure. The type II single crystals were heated at 1623 K for 10 min and then water-quenched. After thermal treatment, the high-temperature phase of the type II crystals has a two-phase ($\text{B}_2 + \gamma$)-structure [5]. The high-temperature phase of the crystals can directly transform to the L_{10} martensite or via intermediate martensitic phases [5–7]. The electrical resistance method was utilized for determination of the forward transformation start temperature M_s during cooling and the reverse transformation finish temperature A_f during heating (Table 1). Intermediate martensitic transformations were not detected by the electrical resistance method. Mechanical tests in the temperature interval $300\text{ K} \leq T \leq 673\text{ K}$ were conducted in vacuum $\sim 10^{-1}\text{ Pa}$. For test in the temperature interval $77\text{ K} \leq T \leq 300\text{ K}$ liquid nitrogen or a mixture of ethyl alcohol with liquid nitrogen was employed.

3. Experimental results

Fig. 1 displays tensile stress–strain curves for the $[001]$ -oriented type I and type II single crystals. In order to measure the SME magnitude, tensile (or compression) tests at $T \leq M_s$ were interrupted at a given strain, then the load was removed and the

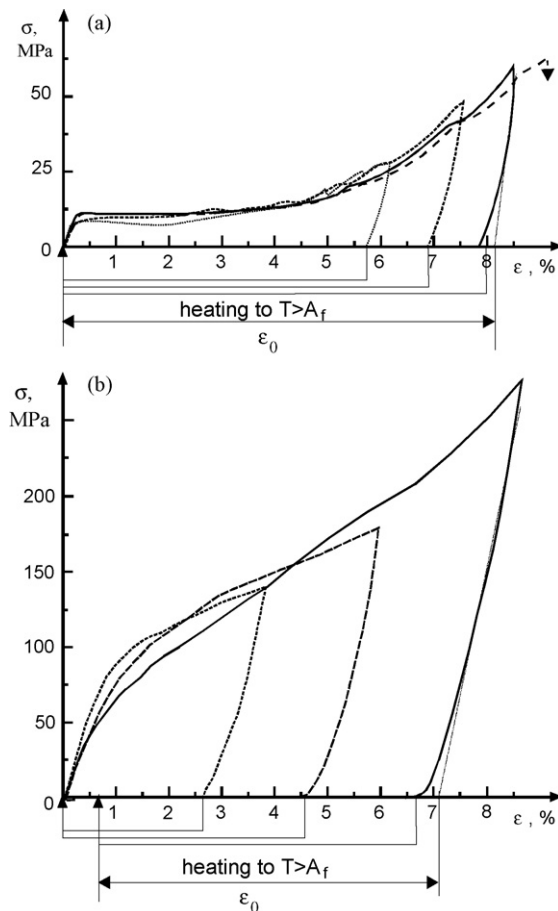


Fig. 1. Cycle loading–unloading curves in $[001]$ oriented type I (a) and type II (b) crystals under tension. Each loading–unloading curve was followed by heating up to $T > A_f$. The maximum recoverable strain ϵ_0 is defined as the magnitude of the SME.

samples were heated to $T > A_f$. The SME strain is defined as the maximal recoverable strain level ϵ_0 obtained. Values of the SME strain for $[001]$ -oriented crystals of type I and II and for $[001]$ -, $[011]$ -, $[\bar{1}23]$ -oriented type III crystals under compression are given in Table 1.

Figs. 2–4 show the SE deformation and the dependence of yield stress ($\sigma_{0.1}$) on test temperature for $[001]$ -oriented crystals of type I (Fig. 2), type II (Fig. 3) under tension/compression and for $[001]$ -, $[011]$ -, $[\bar{1}23]$ -oriented single type III crys-

Table 1
Characteristic temperatures of the $\text{B}_2(\text{L}_{21})$ – L_{10} martensitic transformations and mechanical and functional properties of the type I to III single crystals

| Chemistry (at.%) | M_s (K) | A_f (K) | Orientation | Deformation mode | $\alpha = d\sigma_{0.1}/dT$ (MPa/K) | Temperature interval of SE, ΔT_{SE} (K ± 5 K) | Superelasticity, ϵ_{SE} (% $\pm 0.5\%$) | Shape memory effect, ϵ_0 (% $\pm 0.5\%$) |
|---|-----------|-----------|---------------|------------------|-------------------------------------|---|---|--|
| $\text{Ni}_{54}\text{Fe}_{19}\text{Ga}_{27}$ (type I) | 268 | 281 | $[001]$ | Tension | 1.8 | 390 | 7.0 | 8.1 |
| | | | | Compression | 2.9 | 100 | 4.2 | 5.1 |
| $\text{Co}_{40}\text{Ni}_{33}\text{Al}_{27}$ (type II) | 266 | 298 | $[001]$ | Tension | 0.6 | 220 | 3.9 | 6.5 |
| | | | | Compression | 2.1 | 105 | 2.3 | 3.7 |
| $\text{Co}_{49}\text{Ni}_{21}\text{Ga}_{30}$ (type III) | 235 | 260 | $[001]$ | Compression | 1.0 | 150 | 2.5 | 6.7 |
| | | | $[011]$ | Compression | 2.1 | 130 | 3.8 | 4.9 |
| | | | $[\bar{1}23]$ | Compression | 2.5 | 115 | 2.3 | 4.5 |

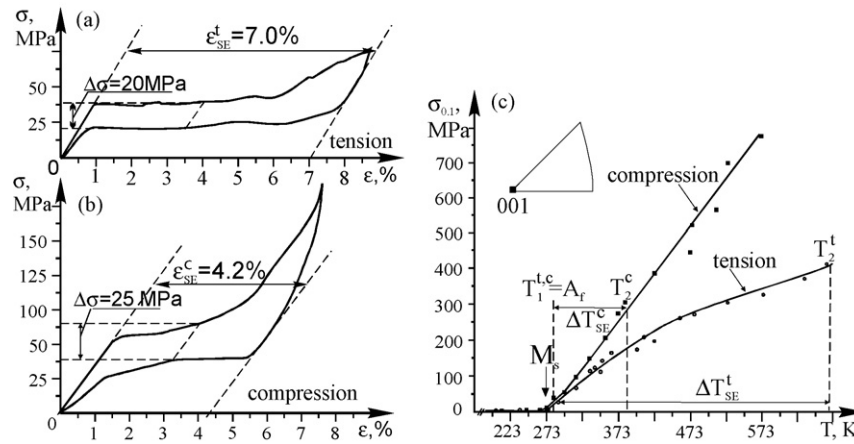


Fig. 2. Deformation behavior of [00 1]-oriented Ni₅₄Fe₁₉Ga₂₇ single crystals under tension and compression: (a) tension SE curve at $T = 284$ K; (b) compression SE curve at $T = 298$ K; $\Delta\sigma$ is mechanical hysteresis; (c) temperature dependence of yield stress $\sigma_{0.1}$; T_1 and T_2 are the temperatures of the onset and the end of the SE temperature interval (ΔT_{SE}) under tension and compression, respectively.

tals (Fig. 4) under compression. The temperature T_1 (the start temperature of SE) was defined as the temperature for the appearance of the first perfect SE loop. The finish temperature of the “SE window” T_2 was determined as the temperature for the appearance of the first open SE loop. The temperature interval of SE is defined as $\Delta T_{SE} = T_2 - T_1$. The strain associated with superelasticity (ϵ_{SE}) was defined as the maximal recoverable strain level during the stress-induced MT. The mechanical hysteresis $\Delta\sigma$ was determined as the stress difference between forward and reverse stress-induced transformation at the middle of the SE curve. Values of ϵ_{SE} and the SE temperature interval ΔT_{SE} for all crystals are summarized in Table 1. In tension along the [00 1] direction, SME and SE of the type I single crystals are $\epsilon_0 = (8.1 \pm 0.5)\%$, $\epsilon_{SE} = (7.0 \pm 0.5)\%$. In compression the corresponding values ($\epsilon_0 = (5.1 \pm 0.5)\%$ and $\epsilon_{SE} = (4.2 \pm 0.5)\%$) are significantly lower than those obtained in tension. The experimentally observed values for ϵ_0 in tension and compression coincide with the theoretical values of lattice deformation of the L₂₁(B2)–L₁₀ MT for the [00 1] orientation ($\sim 9\%$ in tension, $\sim 5\%$ in compression [5,8]). In [00 1]-oriented type II crystals the values of $\epsilon_0 = (6.5 \pm 0.5)\%$ and $\epsilon_{SE} = (3.9 \pm 0.5)\%$ in tension

are lower than in the type I crystals. This is attributed to and the presence of γ -phase precipitations in the type II crystals that do not undergo a martensitic transformation.

For all investigated crystals, the temperature dependence $\sigma_{0.1}(T)$ can be divided into three regimes (Figs. 2c, 3c, 4d). In the first regime at $T < M_s$, the magnitude of $\sigma_{0.1}$ grows with decrease in test temperature and is connected with the beginning of reorientation of the self-accommodated structure of the L₁₀-martensite into a single crystal of martensite [9]. The minimum value in the $\sigma_{0.1}(T)$ -dependence corresponds to the M_s temperature. Figs. 2c and 4d show that the stress $\sigma_{0.1}(M_s)$ is not dependent on crystal axis orientation and on the stress state. $\sigma_{0.1}(M_s)$ always has a low value of around 4–5 MPa for the type I and type III crystals. In the type II crystals, which contain γ -particles, the corresponding stresses are 28–40 MPa (Fig. 3c). For single-phase Ti-51.0 at.%Ni alloy, the magnitude $\sigma_{0.1}(M_s)$ has been reported to be 170 MPa [10], which is substantially higher than the values for any of the present crystals. This indicates that the friction force associated with the movement of twin boundaries in martensite is much lower in the present crystals than in Ti-51.0 at.% Ni.

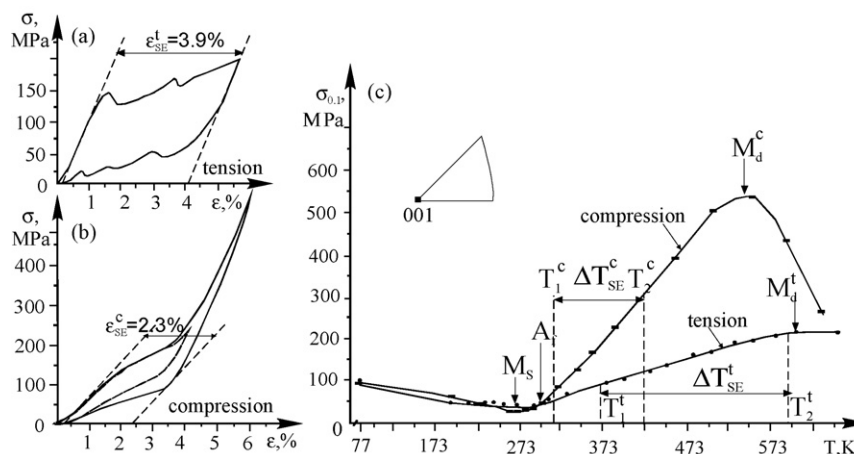


Fig. 3. Deformation behavior of [00 1]-oriented Co₄₀Ni₃₃Al₂₇ single crystals under tension and compression: (a) tension SE curve at $T = 408$ K; (b) compression SE curve at $T = 353$ K; (c) temperature dependence of yield stress $\sigma_{0.1}$.

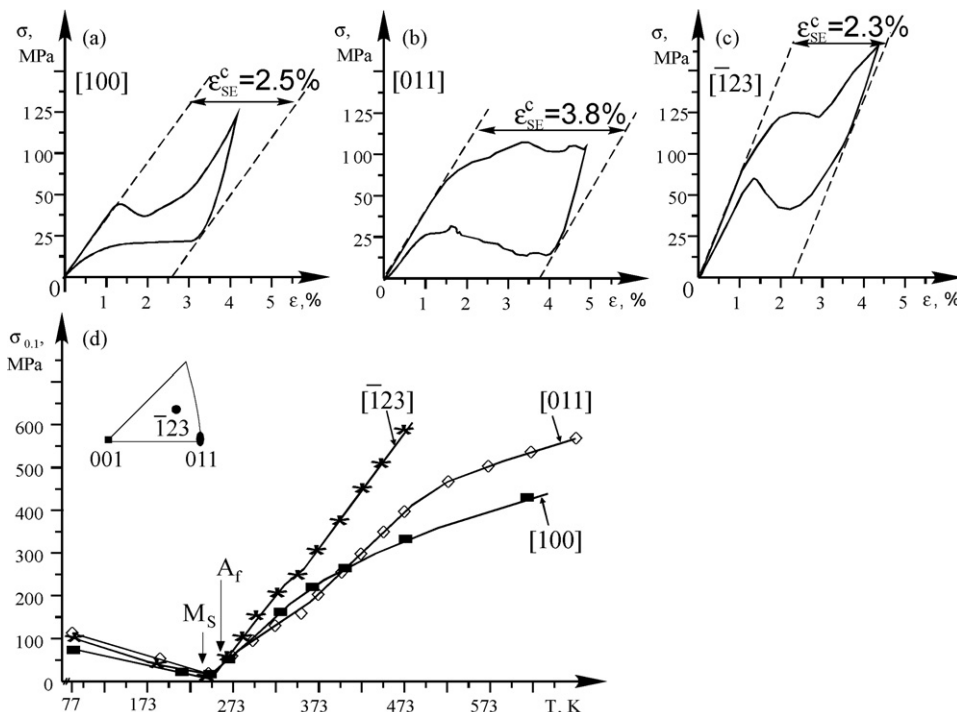


Fig. 4. Orientation dependence of deformation behavior of $\text{Co}_{49}\text{Ni}_{21}\text{Ga}_{30}$ single crystals under compression: (a) SE curve for the $[001]$ orientation at $T=277$ K; (b) SE curve for the $[011]$ orientation at $T=305$ K; (c) SE curve for the $[\bar{1}23]$ orientation at $T=283$ K; (d) temperature dependence of yield stress $\sigma_{0.1}$ for crystals oriented along $[001]$, $[011]$ and $[\bar{1}23]$ directions.

In the second regime at $T > M_s$, the initial crystal structure is the high-temperature phase, and the onset of deformation is associated with stress-induced MT. A linear growth in $\sigma_{0.1}$ with increase in test temperature is found for all orientations under tension and compression and can be described by the Clausius–Clapeyron relationship [9]:

$$\frac{d\sigma_{0.1}}{dT} = -\frac{\Delta H}{\varepsilon_0 T_0}, \quad (1)$$

where ΔH is the enthalpy of transformation, ε_0 the transformation strain and T_0 is the equilibrium temperature for austenite and martensite. In the temperature interval of $M_s < T < M_d$, the magnitude $\alpha = d\sigma_{0.1}/dT$ was found to be dependent on the crystal axis orientation (Fig. 4d) and stress state (Figs. 2c and 3c) for all three crystal types. According to [1], this is associated with the dependence of ε_0 on crystal axis orientation and stress state. The resultant values of ε_0 and α obtained for the present crystals are given in Table 1. The dependencies of ε_0 and α on stress state for type I and II crystals and on the crystal axis orientation for type III crystals are in good agreement with relationship (1): the small values of α correspond to large magnitudes of ε_0 .

For type II crystals, the maximal values of $\sigma_{0.1}$ are found at temperature $T = M_d$. At this temperature the critical stresses for formation of stress-induced martensite and for plastic flow of austenite are equal to each other (Fig. 3c). At $T > M_d$ a normal $\sigma_{0.1}(T)$ -dependence is observed, i.e. the yield stress $\sigma_{0.1}$ decreases with increasing test temperature, and thus, the third regime is associated with the plastic flow of the high-temperature phase. A strong dependence of the strength properties of the B2-phase on stress state was established for

the type II crystals, i.e. $\sigma_{0.1}(M_d) = 550$ MPa under compression and $\sigma_{0.1}(M_d) = 200$ MPa under tension (Fig. 3c). The difference in M_d under compression (523 K) and under tension (600 K) is due to the dependence of α and $\sigma_{0.1}(B2)$ on the stress state. For type I and type II crystals, M_d temperature was not yet reached at $T \leq 673$ K (Figs. 2c and 4d).

The combination of low $\sigma_{0.1}(M_s)$ for the martensitic phase and high yield stress for austenite in all the single crystals provide for superelasticity in a wide temperature interval ΔT_{SE} (Table 1). For the temperature corresponding to the first perfect SE loop occurrence (T_1) and ΔT_{SE} were found to be dependent both on crystal orientation and stress state. For $[001]$ -oriented type III crystals, the small magnitude of mechanical hysteresis $\Delta\sigma = 30$ MPa is the primary cause for SE occurrence at $T_1 = A_f$. In the $[011]$ -oriented type III crystals the magnitude of mechanical hysteresis grows up to $\Delta\sigma = 104$ MPa, and SE was found at $T_1 = A_f + 35$ K. For $[\bar{1}23]$ type III crystals, $\Delta\sigma$ is reduced to 90 MPa and SE was observed at $T_1 = A_f + 20$ K (Fig. 4 a,b,c, Table 2). For $[001]$ -oriented type II crystals SE was found at $T_1 = A_f + 75$ K = 373 K under tension and at $T_1 = A_f + 20$ K = 318 K under compression (Fig. 3, Table 2). The magnitudes of mechanical hysteresis under tension and compression of $[001]$ -oriented type II crystals are close to each other $\Delta\sigma = 100$ –110 MPa (Figs. 3a and b). For the $[001]$ -oriented type I crystals, SE is observed at $T_1 \approx A_f$ both under tension and compression. These crystals also have a small mechanical hysteresis $\Delta\sigma = 20$ –25 MPa (Figs. 2a and b). For the first time, the SE has been observed at temperatures $T > 350$ K in crystals that display the thermoelastic MT. In $[001]$ -oriented type II crystals the temperature interval of SE (ΔT_{SE}) reaches 220 K under tension,

Table 2
Theoretical and experimental values of critical stress, hysteresis and SE start temperature for the type I to III single crystals

| Chemistry (at.%) | Deformation mode | Orientation | Theoretical values | | Experimental values | | | |
|---|------------------|-----------------|-------------------------------------|--------------------------|---------------------|-----------------------------------|---------------------------|------------------------|
| | | | $\Delta\sigma_{\text{theor}}$ (MPa) | T_1^{theor} (K) | σ_0 (MPa) | $\Delta\sigma_{\text{exp}}$ (MPa) | $\sigma_{0.1}(T_1)$ (MPa) | T_1^{exp} (K) |
| Ni ₅₄ Fe ₁₉ Ga ₂₇ (type I) | Tension | [0 0 1] | 35 | $A_f + 2$ | 4 | 20 | 26 | A_f |
| | Compression | | 45 | $A_f + 1.5$ | 4 | 25 | 35 | A_f |
| Co ₄₀ Ni ₃₃ Al ₂₇ (type II) | Tension | [0 0 1] | 103 | $A_f + 70$ | 42 | 110 | 93 | $A_f + 75$ |
| | Compression | | 123 | $A_f + 13$ | 28 | 100 | 105 | $A_f + 20$ |
| Co ₄₉ Ni ₂₁ Ga ₃₀ (type III) | Compression | [0 0 1] | 42 | $A_f + 5$ | 5 | 30 | 60 | A_f |
| | Compression | $[\bar{1} 2 3]$ | 119 | $A_f + 10$ | 5 | 90 | 105 | $A_f + 25$ |
| | Compression | [0 1 1] | 147 | $A_f + 35$ | 5 | 104 | 110 | $A_f + 45$ |

and in [0 0 1]-oriented type I crystals it widens to $\Delta T_{\text{SE}} = 390$ K under tension. This allows for the observation of SE at temperatures up to 670 K (Figs. 2c and 3c). The temperature interval of SE for [0 0 1]-oriented type I and II crystals in compression is $\Delta T_{\text{SE}} = 100$ K (Figs. 2c and 3c).

4. Discussion of results

For the first time, it was experimentally observed that the temperature T_1 of the first open SE loop occurrence depends on crystal orientation and stress state for crystals undergoing stress-induced MT (Figs. 2–4). The analysis of thermoelastic martensitic transformations shows that at $T \geq A_f$ the stress-induced martensite is thermodynamically unstable, so it disappears upon unloading, and the crystal recovers its initial form [9, 11]. According to Liu and Galvin [11], the stress for the forward stress-induced martensitic transformation σ^f is

$$\sigma^f = \sigma_0 + (T - M_s) \frac{d\sigma}{dT}, \quad (2)$$

where σ_0 is the yield stress at $T = M_s$, T the test temperature and $d\sigma/dT$ represent the dependence of yield stress on temperature in accordance with (1). If the resistance to the movement of interphase boundaries is σ_0 and the value of $\alpha = d\sigma/dT$ is equal for both the forward and the reverse MT, then the critical stress for the reverse transformation can be written as [11]

$$\sigma^r = \sigma_0 + (T - A_f) \frac{d\sigma}{dT} \quad (3)$$

In this case the mechanical hysteresis is obtained as

$$\Delta\sigma = \sigma^f - \sigma^r = 2\sigma_0 + (A_f - M_s) \frac{d\sigma}{dT} = 2\sigma_0 + \Delta T \frac{d\sigma}{dT}, \quad (4)$$

where $\Delta T = A_f - M_s$ is the thermal hysteresis. The temperature T_1 is determined not only by condition the $T \geq A_f$, but also by the correlation between yield stress for stress-induced martensite $\sigma_{0.1}$ and the value of the mechanical hysteresis $\Delta\sigma$ [11]:

$$\sigma_{0.1}(T_1) > \Delta\sigma = 2\sigma_0 + \Delta T \frac{d\sigma}{dT}. \quad (5)$$

The temperature T_1 is then determined from the condition $\sigma^r > 0$:

$$T_1 > A_f + \sigma_0 \frac{dT}{d\sigma} \quad (6)$$

Using the relationships (5) and (6) the theoretically calculated magnitudes of the mechanical hysteresis $\Delta\sigma_{\text{theor}}$, and the temperature T_1^{theor} that are necessary for occurrence of SE in the present single crystals are in close agreement with experimental data (Table 2). The analysis of relationships (5) and (6) shows that for SE at $T = A_f$ it is necessary to have low values of σ_0 , $dT/d\sigma = -(\varepsilon_0 T_0)/\Delta H$ and small mechanical hysteresis $\Delta\sigma$. This is experimentally observed in the [0 0 1]-oriented type I crystals in tension/compression and in the [0 0 1]-oriented type III crystals in compression (Table 2). The dependencies of SE start temperature T_1 on crystal axis orientation in the type III single crystals and on stress state in the [0 0 1]-oriented type II crystals are caused by the dependence of $\alpha = d\sigma/dT$ on orientation and stress state (Figs. 2–4, Tables 1 and 2). For example, in the [0 0 1]-oriented type II single crystals under compression the low SE start temperature $T_1 = A_f + 20 = 318$ K is associated with the fact that the necessary level of critical stress for occurrence of complete SE $\sigma_{0.1} > 100$ MPa exceeds the value of the mechanical hysteresis $\Delta\sigma$ and is also reached at lower temperatures than in the samples tested under tension at $T_1 = A_f + 75 = 373$ K (Fig. 3c). The SE finish temperature T_2 is defined as the temperature where the yield stress becomes so high that the growth of martensite is accompanied by generation of the defects, which then impede the reverse MT. For type I and type II single crystals under compression, $\alpha = d\sigma_{0.1}/dT$ is higher than under tension (Table 1). Therefore, the yield stress $\sigma_{0.1}$ for local plastic flow under compression is reached at lower temperatures than in tension. As a result, a reduction of the SE window down to $\Delta T_{\text{SE}} = 100$ K in type I crystals and to $\Delta T_{\text{SE}} = 105$ K in type II crystals under compression was found, whereas this value under tension is equal to $\Delta T_{\text{SE}} = 390$ K in the type I crystals and $\Delta T_{\text{SE}} = 220$ K in the type II crystals (Table 1).

5. Conclusions

- (i) It has been shown that [0 0 1]-oriented Ni₅₄Fe₁₉Ga₂₇ and Co₄₀Ni₃₃Al₂₇ (at.%) single crystals possess a good ductility as compared to brittle Ni₅₀Mn₂₅Ga₂₅ alloys and can yield large strains tension in the temperature interval 77–673 K.
- (ii) For ferromagnetic Ni₅₄Fe₁₉Ga₂₇, Co₄₀Ni₃₃Al₂₇ and Co₄₉Ni₂₁Ga₃₀ single crystals the temperature dependence of the yield stress ($\sigma_{0.1}$) for the stress-induced transformation in the temperature range $M_s < T < M_d$ can be described

by the Clausius–Clapeyron relationship. The magnitude $\alpha = d\sigma_{0.1}/dT$ is found to be dependent on crystal axis orientation, stress state and transformation strain ε_0 .

- (iii) The SE start temperature T_1 was found to depend on crystal axis orientation, stress state and the magnitude of mechanical hysteresis in the single crystals. The onset of SE at $T_1 = A_f$ requires small mechanical hysteresis ($\Delta\sigma \leq 30$ MPa) and high values $\alpha = d\sigma_{0.1}/dT$. A combination of high values of $\Delta\sigma$ (≥ 90 MPa) and small magnitudes of α results in growth of the T_1 temperature to $T_1 = A_f + \Delta$. The maximal value of Δ (75 K) was observed in [001]-oriented $\text{Co}_{40}\text{Ni}_{33}\text{Al}_{27}$ crystals under tension.
- (iv) For the [001]-oriented $\text{Ni}_{54}\text{Fe}_{19}\text{Ga}_{27}$ and $\text{Co}_{40}\text{Ni}_{33}\text{Al}_{27}$ single crystals, high-temperature SE has been experimentally established for tension loading at $T > 400$ K. It was shown that the SE temperature can be controlled by variation of the stress state.

Acknowledgments

This work was supported through the following research grants: CRDF, RUE1-2690-TO-05, RFBR, 05-08-17915, 06-06-08-08011 and fund of “Ausferr”.

References

- [1] H.E. Karaca, I. Karaman, B. Basaran, Y.I. Chumlyakov, H.J. Maier, *Acta Mater.* 54 (2006) 233–245.
- [2] M.A. Marioni, R.S. O’Handley, S.M. Allen, S.R. Hall, D.I. Paul, M.L. Richard, J. Feuchtwanger, B.W. Peterson, J.M. Chambers, R. Techapiesancharoenkij, *J. Magn. Magn. Mater.* 290–291 (2005) 35–41.
- [3] P. Müllner, V.A. Chernenko, G. Kostorz, *J. Magn. Magn. Mater.* 267 (2003) 325–334.
- [4] Y.I. Chumlyakov, I.V. Kireeva, I. Karaman, E.Y. Panchenko, E.G. Zakharova, A.V. Tverskov, A.V. Ovsyanikov, K.M. Nazarov, V.A. Kirillov, *Russ. Phys. J.* 47 (2004) 893–912.
- [5] R.F. Hamilton, H. Sehitoglu, C. Efstathiou, H.J. Maier, Y. Chumlyakov, X.Y. Zhang, *Scripta Mater.* 53 (2005) 131–136.
- [6] K. Oikawa, T. Ota, Y. Sutou, T. Ohmori, R. Kainuma, K. Ishida, *Mater. Trans. JIM* 43 (2002) 2360–2362.
- [7] V.A. Chernenko, J. Pons, E. Cesari, I.K. Zaslachuk, *Scripta Mater.* 50 (2004) 225–229.
- [8] H.E. Karaca, I. Karaman, Y.I. Chumlyakov, D.S. Lagoudas, X. Zhang, *Scripta Mater.* 51 (2004) 261–266.
- [9] K. Otsuka, C.M. Wayman, *Shape Memory Materials*, Cambridge University Press, Cambridge, UK, 1998, p. 284.
- [10] Y.I. Chumlyakov, E.Y. Panchenko, I.V. Kireeva, S.P. Efimenko, V.B. Aksenov, H. Sehitoglu, *Doklady Phys.* 48 (2003) 34–37.
- [11] Y. Liu, S.P. Galvin, *Acta Mater.* 45 (1997) 4431–4439.